Contact Front Phenomena in an Electromagnetic Shock Tube

G.D. Cormack

IPP 3/1o Dezember 1963

INSTITUT FÜR PLASMAPHYSIK

GARCHING BEI MÜNCHEN

INSTITUT FÜR PLASMAPHYSIK

GARCHING BEI MÜNCHEN

Contact Front Phenomena in an Electromagnetic Shock Tube

G.D. Cormack

IPP 3/10 Dezember 1963

Die nachstehende Arbeit wurde im Rahmen des Vertrages zwischen dem Institut für Plasmaphysik GmbH und der Europäischen Atomgemeinschaft über die Zusammenarbeit auf dem Gebiete der Plasmaphysik durchgeführt.

ZUSAMMENFASSUNG

Die Untersuchung der Leuchterscheinungen, der Elektronendichte und -temperatur und der Zeit, nach der Elektrodenmaterial in der stossgeheizten Zone des Plasmas in einem T-Rohr auftritt, lässt erkennen, dass unter den gewählten experimentellen Bedingungen das Leuchten in dieser Zone im wesentlichen von Plasma emittiert wird, das die Kontaktfläche passiert hat.

Eine plausible Erklärung für diesen Prozess der Durchmischung von Entladungsplasma und Gas, das in der Stossfront aufgeheizt wurde, wird diskutiert. Die vermutete Instabilität der Stossfront durch Trägheitseffekte kann die zur Deutung herangezogene Strahlungsabsorption im Gas vor der Leuchtfront ersetzen, mit der von vielen Autoren die in elektromagnetischen Stosswellenrohren gemessenen hohen Temperaturen und anomalen Elektronendichten bisher erklärt wurden.

ABSTRACT

An investigation of the luminosity structure, electron density, temperature, and arrival time of electrode material in the shock heated region of the plasma produced in a T-tube has disclosed that for the conditions studied the luminosity from this region originates primarily from gases that have passed through the contact surface. A plausible explanation for this mixing of discharge gases with shock heated gas is discussed. The proposed inertial instability of the contact front is an alternative explanation rather than radiation absorption in the gas ahead of the luminous plasma for the high values of temperature and anomalous values of electron density that have been measured in electromagnetic shock tubes by numerous workers.

TABLE OF CONTENTS

INTRODUCTION

For high Mach numbers and an initial pressure of the order of 1 mm Hg Cloupeau[1] has shown that most of the luminosity in an electromagnetic H-shaped shock tube originates from the plasma produced by the driving current and not from gases that are shock heated. This conclusion is in agreement with the work of Jeanmaire, Klingenberg and Reichenbach[2] and of Barnard and Cormack[3]. Chang[4] has shown that the distance required for dissociative equilibrium to be reached is long, typically o.4 to 4 cm for a M25 shock passing into un-preexcited hydrogen at an initial pressure of o.2 mm Hg. McLean, Faneuff, Kolb and Griem[5] have explained their much shorter observed times to reach equilibrium as being due to the absorption of radiation in the gas in front of the shock. Brederlow[6] has determined the position of the contact front and has observed luminosity emanating from the shock-heated region in hydrogen in a T-tube. The object of the present work is to extend Brederlow's investigations by making a spectroscopic study of the plasma produced under transition conditions when the gas in the shock heated region is becoming luminous. Spectroscopic methods described by Griem[7] and the method of determination of the source of the plasma, based on the arrival time of certain impurities (Nagakawa and Earnshaw[8]), are used. The effect of the heavy particles introduced by the driving discharge (Cormack[9]) on the motion of the contact front is considered. The results are suggestive of an alternative mechanism to that proposed by McLean, Faneuff, Kolb and Griem[5] that would explain the short time to reach equilibrium and the high value of temperature and anomalous values of electron density that have been measured by numerous workers using electromagnetic shock tubes. The mechanism that is proposed is in agreement with the work of Cloupeau[1].

APPARATUS

The T-type shock tube used had an internal diameter of 3o mm and contained 6 cm long electrodes of the same design as those used by Brederlow[6]. The V x B electrodes and wire net used by Brederlow[6] were omitted. A 7.8 μF capacitor was used as a current source and a 8 mm diameter 19 cm long carbon rod of d.c. resistance 13o milliohms was mounted as near as possible to the rear of the electrodes to serve as a back-strap and as a damping resistance. The current waveform observed with a Rogowski coil encircling one arm of the T-tube was nearly critically damped and had only one overshoot. Current observations* were made at shock tube pressures of o.1, o.25, 2.5 and 9.8 mm Hg of Hydrogen and capacitor voltages of 7, 1o and 14 kV. The maximum value of the current increased slightly when the initial pressure in the shock tube was increased. The ratio of the amplitude of the second current pulse to the first was 1/5 and the duration of the first current pulse was 3.9 to 4.15μsec, the higher value being observed for low initial pressures and low capacitor voltages. The position of a small abrupt increase in the magnitude of dI/dt was observed at times of from o.36 to 2.6μsec after the current had started to flow. The lower value was observed when the pressure in the shock tube was o.1 mm Hg and the capacitor voltage 14 kV and the higher value at a pressure of 9.8 mm Hg and a capacitor voltage of 7kV. From the observed dependency of this time on the initial pressure in the shock tube and on the capacitor voltage, it could be concluded that this discontinuity in dI/dt was probably caused by the stopping of the axial motion of the current path between the electrodes. Such a conclusion is supported from simple acceleration theory by both the sign and the magnitude of the observed increase in dI/dt. Theory predicts that $\Delta(dI/dt) \approx -L_1 I\ \Delta(dx/dt)/(L_o+L_1 x)$ where $\Delta(dI/dt)$ is the increase in dI/dt at the time $t=\tau$ that is caused by a sudden decrease in the current sheet velocity of an amount $\Delta(dx/dt)$. L_1 is the inductance per unit length of the driver. L_o is the time-independant inductance of the driving circuit and x is the distance that the current sheet has travelled down the tube at time $t=\tau$. This equation is valid only for a brief time after $t=\tau$. From the known circuit parameters and the values observed for t, the distance that the driving current moved down the tube could be calculated from simple acceleration

theory (Cormack[9], equation 5) to be always of the order of magnitude of the electrode length. This value is in agreement with the work of Muntenbruch[10]. He determined with magnetic probes that the driving arc does not go down a T-tube a distance past the electrodes of greater than about one tube diameter. It was concluded from the current measurements that the driving discharge did not travel down the tube to the location where spectroscopic observations were made, which was at x=24 cm from the center of the arms of the T-tube. At a pressure of 2.5 mm Hg and a capacitor voltage of 10 kV, the plasma arrived at x=24 cms 8.6 μsec after the current started to flow. When the capacitor was discharged from 13 kV the plasma took 6.8 μsec to travel to the observation point. Thus all spectroscopic measurements were made at a time when major magnetohydrodynamic effects due to the driving current were small. It is of further interest to note that the preceding measurements show that the ρ_1/ρ_0 data of Brederlow[6] should be multiplied by a factor of about 0.6. The corrected ρ_1/ρ_0 curves are then in close accord with snowplough theory, for a shock moving into gas that is not pre-excited.

A Steinheil f/10 three-glass-prism spectroscope equipped with either a mounting for photographic plate or a four-photomultiplier adaptor was used for the spectroscopic measurements. A limited amount of information on the spatial distribution of the plasma luminosity transverse to the axis of the tube could be obtained because two photomultipliers received radiation from a region 2 mm high and a fraction of a mm wide and the other two photomultipliers from a region of the same size but displaced by 3 mm in a direction transverse to the axis of the tube. Similarly each line in the time-integrated spectra recorded on photographic plates was due to the radiation coming from a region in the plasma 5 mm high with a blank region in the middle of height 1 mm. The blank region was caused by an aperture inserted at the entrance slit of the spectroscope. The spectral resolution of the spectroscope with the photomultiplier adaptor attached was sufficient to resolve lines at 4300 ^{o}A separated by 0.35 ^{o}A when the entrance and exit slits were 20 μ wide.

The same image convertor camera and rotating mirror camera as used by Brederlow[6] were employed for determining the velocity and the luminosity structure of the plasma.

SPECTROSCOPIC MEASUREMENTS

With hydrogen in the shock tube at an initial pressure of 2.5 mm Hg and 1o kV on the capacitor, the velocity of the luminosity front at x=24 cm was 1.5 cm/μsec. Reflected shock observations with tne image convertor camera and the rotating mirror camera used as a smear camera showed that there was no luminous incident shock in front of the main luminosity. A non-luminous shock-heated region having an axial dimension of less than about 5 mm could however have been present. The accuracy of measurement, about 1 mm, was insufficient to resolve whether or not the incident luminous front reached the reflector plate. At no time was the luminosity immediately in front of the reflector plate observed to be reproducible. A spectroscopic investigation of the plasma within 1 mm of the reflector plate was not attempted both because of the severe spatial requirement and the observed irreproducibility. Brederlow[6] has investigated the properties of the plasma produced under similar conditions. For example, in his Fig.2, picture II, the velocity of the first luminosity front is 1.67 cm/μsec and the initial pressure 2.5 mm Hg. For these conditions he detected a contact front moving with a velocity of 1.41 cm/μsec at a distance behind the first luminosity front of about 8.6 mm. It is of interest to determine the state of the plasma both in front of and behind this contact front. Thus electron density n_e measurements were made by observing the half-width of the emitted H_β line, temperature T measurements were made by the method described by Griem[7] - by observing the ratio of total H_β intensity to the intensity of the underlying 1oo ^{o}A wide continuum, and the arrival time of the Cr I 4254.35 ^{o}A line was measured. The first two measurements provided information on the state of the luminous plasma and the last the source of the plasma. The source could be pre-excited gas in front of the shock (McLean, Faneuff, Kolb and Griem[5]) or gases from the driving discharge (Cloupeau[1]).

Time integrated spectra of the radiation from the plasma revealed lines of H_β, H_γ and H_δ. When the amount of exposure was increased by using the most sensitive available spectroscopic plates and 2oo firings of the shock tube for each exposure, then H_ϵ and the resonance lines of Cr I, Fe I, Si II and Ca II became just detectable. The metallic lines originated from material coming from the stain-

less steel electrodes and from two set-screws that joined these electrodes to the conductors in the arms of the T-tube.

At a luminosity front velocity of 1.5 cm/μsec the amplitudes of the photomultiplier signals often differed by as much as a factor of two for different firings of the shock tube. Shot-to-shot irreproducibility also affected the shape of the signals. The shape of the signal observed with a photomultiplier viewing a narrow region in the center of the H_β line was identical to that of the signal from a photomultiplier viewing the center of the H_γ line for the same shot when both photomultipliers received light from the same region of plasma. The shape of two such signals often differed considerably when the photomultipliers viewed regions of plasma separated 3 mm in a radial direction. Thus the plasma being studied was markedly inhomogeneous. Therefore the method of measuring spectroscopic quantities was modified to reduce errors caused by this inhomogeneity and the shot-to-shot irreproducibility. For example, all subsequent measurements were made with two photomultipliers that viewed the same region of plasma. Also all measurements were normalized to a simultaneously recorded standard signal. For example, a point on the H_β profile was obtained by simultaneously recording the oscillograms of the signals from two photomultipliers, one viewing the middle of H_γ and the other the radiation in a narrow wavelength interval at the desired wavelength in H_β. The second signal was corrected to a small extent for photomultiplier spectral sensitivity from the manufacturer's data, for spectroscope dispersion and for the underlying continuum signal. This corrected signal within H_β was proportional to the intensity of the radiation in the wavelength interval defined by the slit widths. The continuum signal was measured by recording the signal from a photomultiplier that viewed a 10 ^{o}A interval centered on 5134 ^{o}A. The continuum signal at the desired wavelength within the H_β profile was determined by extrapolating the signal measured at 5134 ^{o}A using the theoretical continuum intensity vs. wavelength relation and appropriate corrections for slit widths, photomultiplier spectral sensitivity and spectroscope dispersion. These corrections were made in this manner since no absolute calibration of the optical system was made. The corrected H_β signal was then divided by the simultaneous-

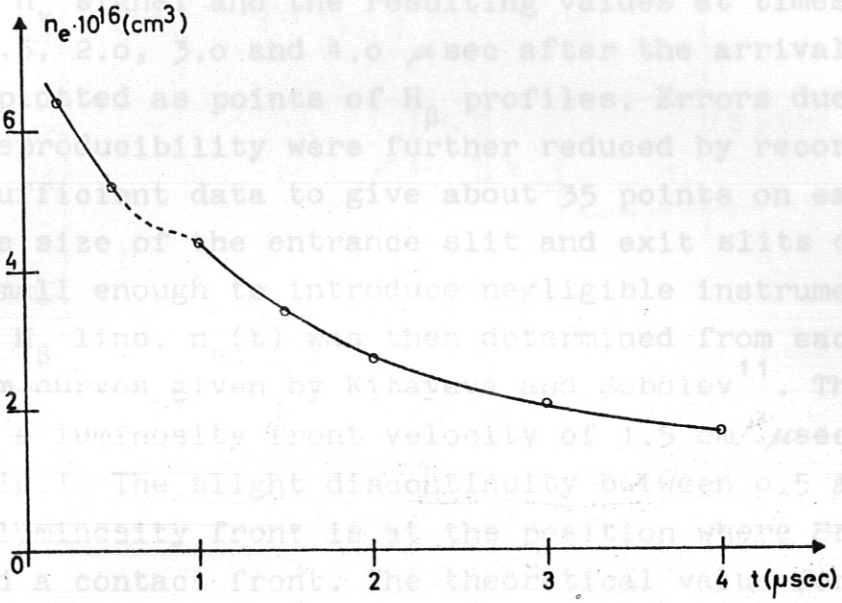

Fig.1 Electron density throughout luminous plasma. The velocity of the luminous front at the observation location, x=24 cm, was 1.5 cm/μsec. t=o defines the arrival of the first luminosity at x=24 cm.

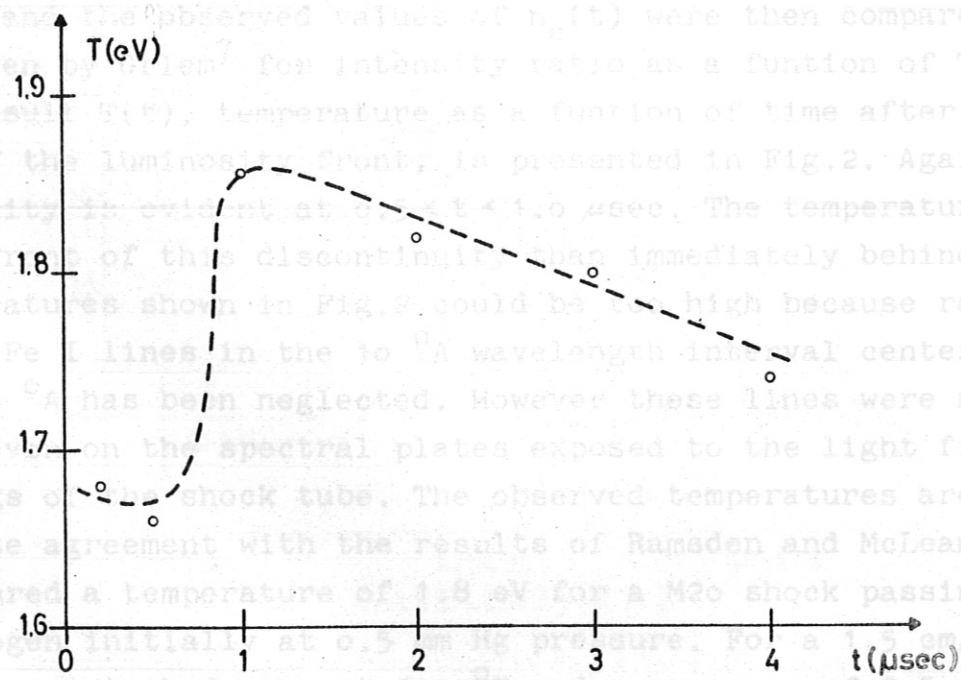

Fig.2 Temperature throughout luminous plasma. Experimental conditions were the same as for Fig.1.

ly observed H_γ signal and the resulting values at times of o.2, o.5, 1.o, 1.5, 2.o, 3.o and 4.o μsec after the arrival of the luminosity plotted as points of H_β profiles. Errors due to shot-to-shot irreproducibility were further reduced by recording and analyzing sufficient data to give about 35 points on each line profile. The size of the entrance slit and exit slits of the spectroscope were small enough to introduce negligible instrument broadening of the H_β line. $n_e(t)$ was then determined from each line profile from curves given by Kitayeva and Sobolev[11]. The $n_e(t)$ results for a luminosity front velocity of 1.5 cm/μsec are presented in Fig.1. The slight discontinuity between o.5 and 1.o μsec behind the luminosity front is at the position where Brederlow[6] has observed a contact front. The theoretical value for n_e at equilibrium behind a shock having a front velocity of 1.5 cm/μsec and moving into unexcited hydrogen at 3oo ^oK and 2.5 mm Hg pressure is less than $1o^{13}$ / cm^3. Thus the observed value for n_e, $\sim 1o^{16}$ /cm^3, is considerably higher than that directly due to shock heating.

The temperature measurements were made by first integrating each observed H_β line profile to obtain the total line intensity then dividing by the extrapolated value of the continuum signal noted above. The observed ratios of line intensity to 1oo ^oA continuum intensity and the observed values of $n_e(t)$ were then compared with curves given by Griem[7] for intensity ratio as a funtion of T and n_e. The result T(t), temperature as a funtion of time after the arrival of the luminosity front, is presented in Fig.2. Again a discontinuity is evident at $o.5 < t < 1.o$ μsec. The temperature is lower in front of this discontinuity than immediately behind it. The temperatures shown in Fig.2 could be too high because radiation from weak Fe I lines in the 1o ^oA wavelength interval centered about 5134 ^oA has been neglected. However these lines were never observed even on the spectral plates exposed to the light from 2oo firings of the shock tube. The observed temperatures are in approximate agreement with the results of Ramsden and McLean[12]. They measured a temperature of 1.8 eV for a M2o shock passing into hydrogen initially at o.5 mm Hg pressure. For a 1.5 cm/μsec shock moving into hydrogen at 3oo ^oK and a pressure of 2.5 mm Hg the temperature predicted from shock theory is o.35 eV. Thus the measured temperature throughout the luminous plasma is higher than that predicted by the theory for a shock moving into unexcited,

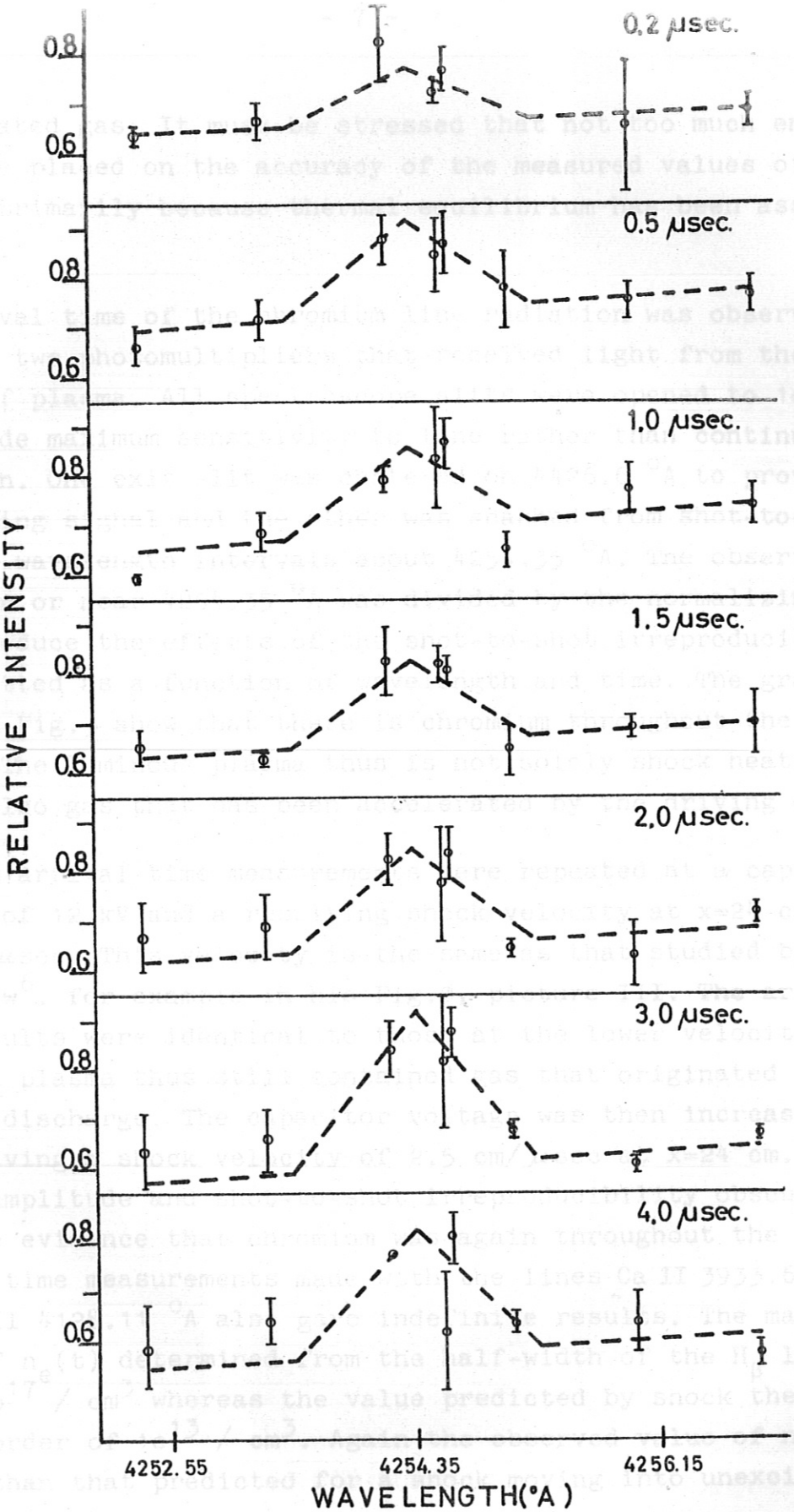

Fig.3 Detection of Cr I 4254.35 °A. Slit widths were of such a size that the luminosity width in these graphs should ideally be 1.8 °A wide and of the triangular shape shown. Experimental conditions were as in Fig.1. The ordinate of each graph is the ratio of the signal observed near 4254.35 °A to a normalizing signal at 4426.6 °A. Each point is the mean value of up to 8 observations and each error bracket denotes the standard error of the mean.

un-preheated gas. It must be stressed that not too much emphasis should be placed on the accuracy of the measured values of temperature, primarily because thermal equilibrium has been assumed to exist.

The arrival time of the chromium line radiation was observed with the two photomultipliers that received light from the same region of plasma. All spectroscope slits were opened to 100 μ to provide maximum sensitivity to line rather than continuum radiation. One exit slit was centered on 4426.6 ^{o}A to provide a normalizing signal and the other was scanned from shot-to-shot in small wavelength intervals about 4254.35 ^{o}A. The observed signal on or near 4254.35 ^{o}A was divided by the normalizing signal to reduce the effects of the shot-to-shot irreproducibility, then plotted as a function of wavelength and time. The graphs shown in Fig.3 show that there is chromium throughout the luminous plasma. The luminous plasma thus is not solely shock heated gas but is also gas that has been accelerated by the driving discharge.

Chromium arrival time measurements were repeated at a capacitor voltage of 12 kV and a resulting shock velocity at x=24 cm of 2.0 cm/μsec. This velocity is the same as that studied by Brederlow[6], for example in his Fig.2, picture III. The arrival time results were identical to those at the lower velocity. The luminous plasma thus still contained gas that originated from the driving discharge. The capacitor voltage was then increased to 13 kV giving a shock velocity of 2.5 cm/μsec at x=24 cm. Small signal amplitude and shot-to-shot irreproducibility obscured any positive evidence that chromium was again throughout the plasma. Arrival time measurements made with the lines Ca II 3933.67 ^{o}A and Si II 4128.11 ^{o}A also gave indefinite results. The maximum value of $n_e(t)$ determined from the half-width of the H_β line was 1.2×10^{17} / cm^3 whereas the value predicted by shock theory is of the order of 10^{13} / cm^3. Again the observed value of n_e was higher than that predicted for a shock moving into unexcited, un-preheated gas.

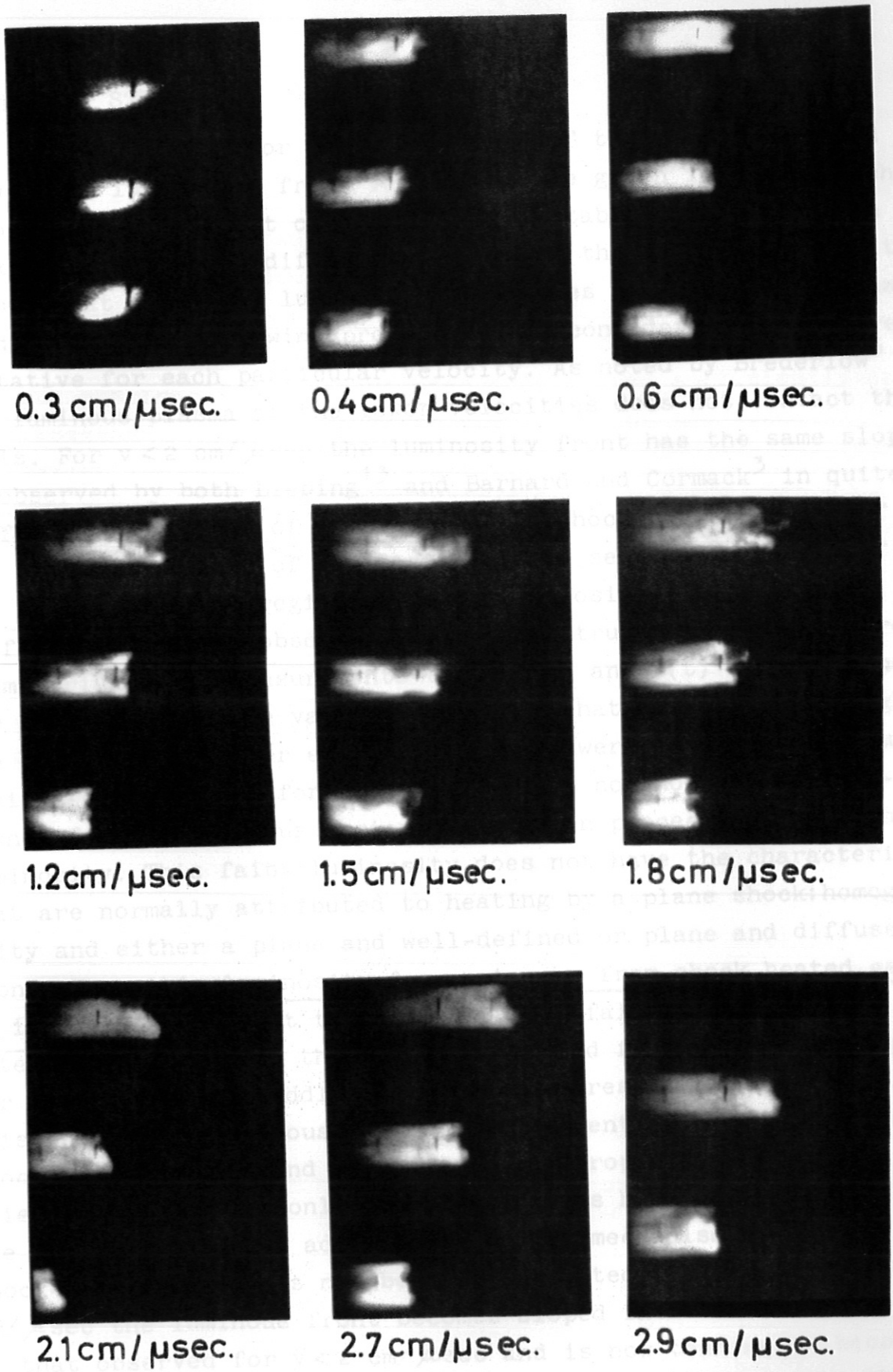

Fig.4 Luminosity structure of plasma. Fiducial marks are at x=19, 22 and 25 cm. Luminosity front velocities at x=24 cm are given. Each set of two or three pictures is of the same plasma and the delay time between each picture is 1.2 μsec. The initial pressure in the shock tube was 2.5 mm Hg and different velocities were obtained by varying the capacitor charging voltage. The left side of each picture is cut off by a diaphragm and the different vertical spacings between pictures does not affect the magnification.

LUMINOSITY STRUCTURE

Typical image convertor camera pictures of the plasma produced at various luminosity front velocities are given in Fig.4. Each velocity given is that of the first detectable luminous region at x=24 cm. Although different firings of the shock tube resulted in somewhat different luminosity structures for the same discharge conditions, the following properties are considered to be representative for each particular velocity. As noted by Brederlow[6] the luminous plasma at the lower velocities does not contact the walls. For $v < 2$ cm/μsec the luminosity front has the same slope as observed by both Liebing[13] and Barnard and Cormack[3] in quite different geometries of electromagnetic shock tubes. In all of the pictures regions of luminosity can be seen moving ahead of and faster than the region of major luminosity. In particular, it follows from the observed luminosity structures and the chromium arrival time measurements that $n_e(t)$ and $T(t)$ in Fig.1 and 2 for $o < t < 1$ μsec are values for plasma that has passed through the contact front. For example, in the lower picture of the luminosity that is shown for v=1.5 cm/μsec a non-homogenous, non-plane, faintly luminous region can be seen preceeding the main luminosity. This faint luminosity does not have the characteristics that are normally attributed to heating by a plane shock: homogeneity and either a plane and well-defined or plane and diffuse front. Thus this luminosity does not come from shock heated gas. It is also of interest to note that this faint region is not detectable later when the plasma has moved further down the tube, for example in the middle and upper pictures at this velocity. This previously luminous gas must be present in the non-luminous shock-heated region and must affect the properties of the gas in this region. Because only luminous plasmas have been studied in the present work this additional heating mechanism of non-luminous shock-heated gases has not been investigated further. For $v \geq 2$ cm/μsec the luminous front becomes sloped in a direction opposite to that observed for $v < 2$ cm/μsec and is now tending to become well-defined. However the slope of this front increases as the plasma moves down the tube. Thus there is still some mechanism present that is preventing the usual stabilizing characteristic of a shock from being operative. The dependancy of the angle of the front on the capacitor voltage could be due to the motion of

a region of heavy particles inside the plasma. The driving current sputters off material from the anode of the driver and any glass subjected to electron bombardment, for example that near the tip of the anode. The heavy ions are then accelerated both down the tube and in a transverse direction. The amount of transverse motion that occurs increases with increasing capacitor voltage. Thus at x=24 cm and at low voltages the region of sputtered material could still be at the top of the tube whereas at higher voltages the region could have been accelerated sufficiently in the transverse direction to be at the bottom of the tube. This explanation for the change in angle is only a proposed explanation. Although the front is non-reproducible and non-plane when $v > 2$ cm/μsec, no regions of plasma were observed to be ejected through the front at these high velocities. Also at these high velocities the plasma was more homogeneous.

Reflected shock pictures revealed a zone of non-luminous shock heated gas in front of the luminous plasma when $v < 1{,}5$ cm/μsec. The accuracy of observation, about 1 mm, was insufficient to resolve whether or not a zone existed at higher velocites. Plots of either arrival time or velocity as a function of capacitor voltage could be assymptotically approximated by two straight lines that intersected at a velocity of about 1.5 cm/μsec. It is concluded that below this velocity a non-luminous shock preceeded the luminous plasma and that for velocities greater than approximately this value the luminosity front coincided with the shock front.

DISCUSSION

The presence of the discharge gases in the region of shock heated gas shows that the enthalpy, pressure and density in the luminous region of the shock heated gas cannot be predicted by the simple Rankine-Hugoniot relations. Rather if one insists on using these relations one must take into account for example the increase in the enthalpy in this region that comes from the energy flow across the contact front. This energy is transfered by radiation, thermal conduction, and mass transfer. The present observations have shown that the flow of high temperature gases through the contact front and their resultant mixing with the shock heated gas is a major contribution to this energy flow. The Rankine-Hugoniot equations could be modified, most simply but not adequately, by introducing one term in the energy equation. This term would be an enthalpy term that would take into acccunt the energy that is transported into the shock heated region by the discharge gases that pass through the contact surface. Such a term would be mathematically equivalent to the radiative energy transfer term that has been proposed by McLean, Faneuff, Kolb and Griem[5] to explain their high temperature and low electron density observations.

Mechanisms such as proposed by Cloupeau[1] will contribute to the spreading out of the contact front. In the present experiments an inertial instability of the contact front can explain the presence of the ionized heavy atoms in the shock heated gas and the observed structures of the luminosity. The passing of regions of plasma through the contact front could be due to not only a non-homogeneous mass density distribution behind the front but also by the motion of regions possessing a higher-than-average momentum. The latter mechanism would account, for example, for the shape of the luminosity front shortly after a second region of plasma accelerated by the second half-cycle of current has overtaken the luminosity front produced by the first half-cycle of current. A typical smear picture showing this phenomenon is given by Cloupeau[1] in his Fig.4. It is believed that this phenomenon is not responsible for the shape of the luminosity front in the present experiments. For example, in the smear pictures given by Brederlow[6] in his Fig.2, II and III, a second faint region of luminosity can be seen about 5 μsec behind the primary front.

This second region is accelerated by the second half-cycle of current, however to a velocity that is insufficient for the overtaking of the primary front. When the plasma behind the contact front has a non-homogeneous mass density distribution, the motion of each small region of non-homogeneity is deceleration dependant. The deceleration of the plasma in an electromagnetic shock tube is usually of the order of 10^{11} cm/sec^2. The deceleration is in such a direction as to favor Rayleigh-Taylor or other inertial instabilities that would develop on the surface of the contact front when the mass density of the gases behind the front exceeds that of those before the front. The marked lack of inhomogeneity behind the contact front for $0.6 < v < 2$ cm/μsec favors the passage of regions of plasma through the front rather than the more-ordered Rayleigh-Taylor instability. Such motion of regions has been recorded in numerous photographs in the present work. The lack of homogeneity and the persistence of the internal structure of the luminosity indicates that mixing through diffusion and turbulence are of minor importance in comparison to mixing that is due to the motion of inhomogeneous regions. The increase in homogeneity observed when $v > 2$ cm/μsec and the smoothing out of the shape of the luminosity front could be explained by enhanced diffusion at the higher temperature and the probable joining together of the shock front with the luminosity front (see also Chang[14]). The persistence of the structure of the luminosity is still evident at these higher velocities. For example, the slope of the front increases as the plasma moves down the tube. This tendency of the front to become less plane as the plasma moves down the tube has also been noted by McLean, Faneuff, Kolb and Griem[5]. The present work indicates that the region immediately behind the luminosity front is partially composed of gases accelerated by the driving discharge. The actual shape of the front would be determined by a balance between the stabilizing effect of the shock (Freeman[15]) and the unstabilizing effect of inertial instabilities. One further noteworthy characteristic introduced by the deceleration of the shock front in an electromagnetic shock tube is the introduction of a deceleration-dependence of the density on the distance from the front. This deceleration-dependency is expressed accurately by blast-wave theory. The magnitude of the inertial effects acting on regions

near the contact surface can be estimated by comparing the scale heights (Opik[16]) of hydrogen and chromium. For example, the scale height for 5,000 ^{o}K hydrogen atoms subjected to a deceleration of 10^{11} cm/sec^2 is 3.2 cm and for gaseous chromium 0.1 cm. The difference in these scale heights indicates that there can be a mass filtering action at the contact front. Heavy particles and/or regions of higher than average value of local mass density can move through the contact front. Since the deceleration of the plasma invariably increases when the velocity of the plasma is increased or when the initial gas pressure is decreased, it follows that the mass filtering action would be more pronounced under conditions of high velocity and low density, the regime of operation that has been of most interest to users of electromagnetic shock tubes.

The instability mechanism that has been proposed could have a wide range of applicability. For example, there have appeared numerous papers dealing with electromagnetically-driven shock waves in which irreproducibility is a common characteristic. Irreproducibility favors the inertial instability explanation for the inapplicability of the simple Rankine-Hugoniot relations rather than the radiative energy transfer mechanism proposed by McLean, Faneuff, Kolb and Griem[5].

It has been established for the conditions studied that the region immediately ahead of the contact front is inhomogeneous and contains high temperature, high electron density gas that originates from behind the contact front. It cannot be concluded that this mixing process occurs under all conditions in electromagnetic shock tubes. For low velocities and high initial pressures Jeanmaire, Klingenberg and Reichenbach[2] have shown that a shock front can exist in a T-tube. The presently proposed instability mechanism could however account for the failure of numerous workers to obtain impurity-free, homogeneous plasmas formed behind plane shock fronts under conditions of low initial pressure and high velocity in electromagnetic shock tubes.

ACKNOWLEDGEMENTS

It is a pleasure to acknowledge the stimulating discussions with Dr.H.Muntenbruch and the suggestions given by Dr.R.Wienecke and Dr.G.Brederlow. Technical assistance has been provided by many persons, notably however by H.Kolig.

This work was supported by the National Research Council of Canada and was a part of a joint research program undertaken by the Institut für Plasmaphysik and Euratom. This work was performed while the author was a guest at the Institut für Plasmaphysik. The author is deeply grateful for the use of experimental facilities and for the technical and scientific assistance provided by the Institut für Plasmaphysik.

APPENDIX I

DYNAMICS DURING ACCELERATION

A complete description of the motion of the plasma and the waveform of the driving current could be determined from a machine solution of the two coupled differential equations governing the system. These equations are typically a circuit and a momentum equation. The major effect on the current waveform of a sudden stopping of the current sheet can be readily found by considering only the circuit equation. Typically this has the form

$$\frac{1}{c}\int_0^t I\,dt + \frac{d}{dt}\left\{(L_0 + L_1 x)\,I\right\} + RI = V_0 \qquad (1)$$

where a discharge circuit consisting of a capacitor c initially charged to a voltage of V_0 passes current I into a resistance R and an inductance L_0+L_1x. L_0 is a time-independant inductance, L_1 is the inductance per unit length of the driver and x is the position of the current sheet relative to the base of the driver. When the current sheet velocity suddenly decreases from a value of $\dot{x}$ to zero, or $\Delta\dot{x}$, then only the term containing the highest order derivative of I responds to the change. Thus if the velocity changes by $\Delta\dot{x}$ at the time $t=\tau$, then for $t=\tau+$, a time immediately after τ, the following equation is valid

$$\left\{L_0 + L_1 x\right\}\Delta\dot{I}(\tau+) + L_1 I\,\Delta\dot{x}(\tau) = 0 \qquad (2)$$

which is the equation given on page 2.

The value of x(t) and $\dot{x}(t)$ from snowplough theory for a damped sinusoidal driving current

$$I = I_0\, e^{-\delta t} \sin \omega t \qquad (3)$$

are from reference 17

$$x(t) = \sqrt{\frac{L_1}{m_1}}\ \frac{I_0}{2}\left\{\frac{\omega^2 t}{\delta[\omega^2+\delta^2]} + \frac{e^{-2\delta t}}{2\delta^2} - \frac{\omega^4+3\omega^2\delta^2}{2\delta^2[\omega^2+\delta^2]^2} + \frac{e^{-2\delta t}}{2[\omega^2+\delta^2]^2}\left\{[\omega^2-\delta^2]\cos 2\omega t + 2\omega\delta \sin 2\omega t\right\}\right\}^{1/2} \quad (4)$$

or

$$x(t) = \sqrt{\frac{L_1}{m_1}}\ I_0\left[\frac{\omega^2 t^4}{12} - \frac{\delta\omega^2 t^5}{10} + \frac{\omega^2 t^6}{90}\left\{6\delta^2-\omega^2\right\} + \frac{\delta\omega^2 t^7}{63}\left\{\omega^2-2\delta^2\right\} + \frac{\omega^4 t^8}{1260}\left\{\omega^4-15\delta^2\omega^2\right\} + \cdots\right] \quad (5)$$

and

$$\dot{x}(t) = \frac{L_1 I_0^2}{8 m_1 x(t)}\left\{\frac{\omega^2}{\delta[\omega^2+\delta^2]} - \frac{e^{-2\delta t}}{\delta} + \frac{e^{-2\delta t}}{\omega^2+\delta^2}\left[\delta\cos 2\omega t - \omega \sin 2\omega t\right]\right\} \quad (6)$$

where m_1 is the mass of the gas per unit length initially in the tube,

$$\omega^2 = \frac{1}{L_0 C} - \delta^2 \quad (7)$$

$$\delta = R/2L_0 \quad (8)$$

and

$$I_0 = V_0 \omega C \quad (9)$$

It is assumed that material from the driving electrodes does not greatly affect the plasma motion. The spectroscopic observations show that there is electrode material in the plasma; however the amount is small and unknown and thus for the present calculations is considered negligible. The assumption that the driving current is a damped sinusoid is made only to simplify the calculations. The value of δ can be determined from the amplitude of successive pulses of the current, ω from the half period, L_0 from equation 7 and I_0 from equation 9. Then assuming that the advancing current sheet picks up all gas that is encountered, $m_1 = \rho_0 A$

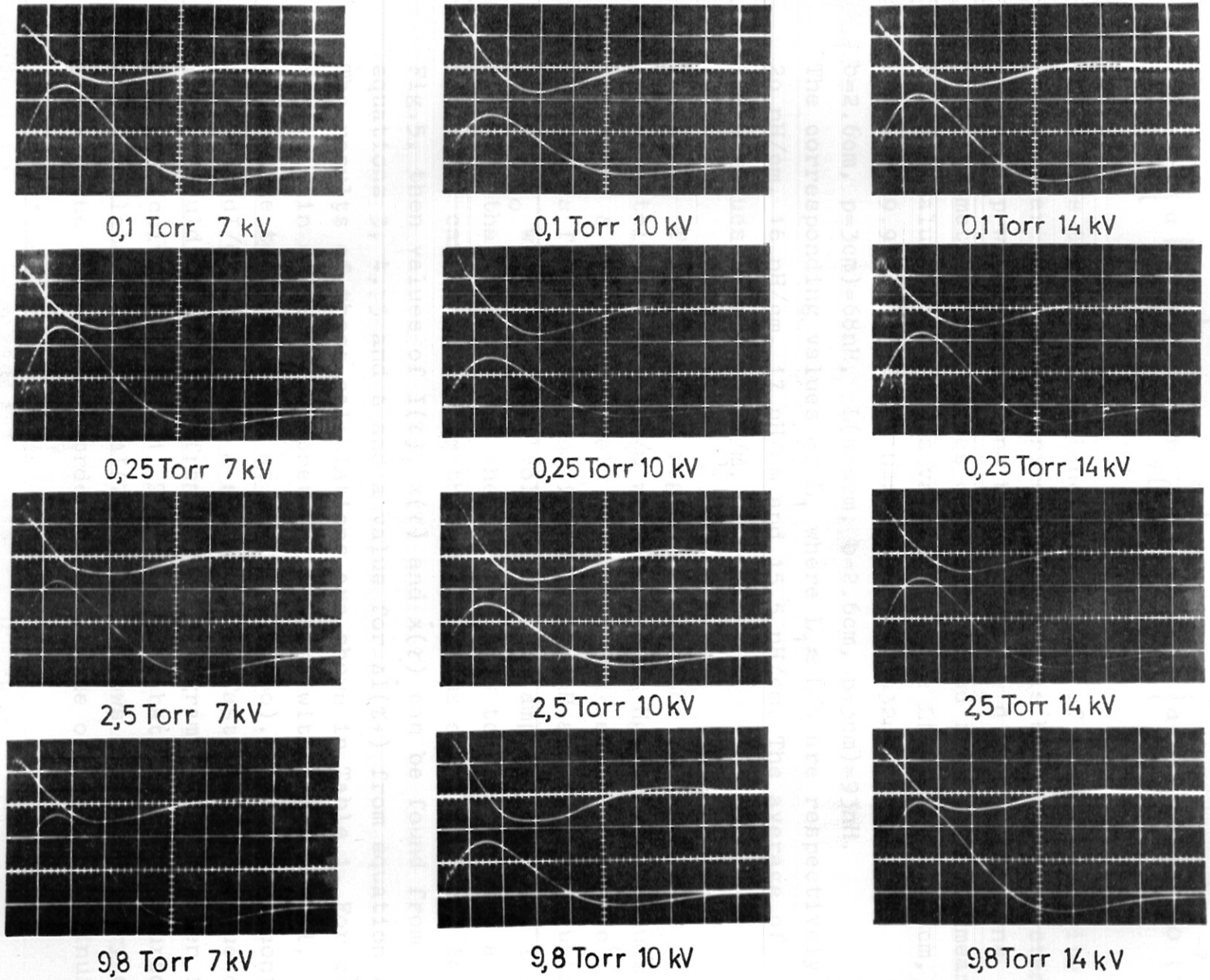

Fig.5 Driving current as a function of initial pressure and capacitor voltage. Each upper waveform is proportional to dI/dt and each lower I. The sweep speed is 1 cm/μ sec.

where A is the cross-sectional area of the region between the electrodes and ρ_o the initial mass density. L_1 can be estimated from an equation given by Gray[18]

$$L \simeq 4\left\{a \ln\frac{4ab}{p(a+d)} + b\ln\frac{4ab}{p(b+d)} + 2d + \frac{1}{2}\left\{a+b\right\} + 0.223p\right\} \times 10^{-7} \quad (10)$$

where L is the self-inductance in henries of a conductor with a rectangular section of perimeter p which is bent into a rectangular loop with sides a and b and diagonal d, all dimensions being in meters. The values of L calculated from measured mean b and p values and various values of a are L(a=.5cm, b=1.6cm, p=4.2cm)=9.9nH, L(a=2cm, b=2cm, p=3.6cm)=32nH, L(a=4cm, b=2.6cm, p=3cm)=68nH, L(a=6cm, b=2.6cm, p=3cm)=93nH. The corresponding values of L_1 where $L_1 \approx L/a$ are respectively 20 nH/cm, 16 nH/cm, 17 nH/cm and 15.5 nH/cm. The average of these values is $1.7 \cdot 10^{-6}$ H/m.

The value for m_1 for the region between the electrodes is approximately $1.95 \cdot 10^{-7}$ kg/m when P_o=2.5 mm Hg. Average values for ω and δ are respectively $0.781 \cdot 10^{6}$ rad/sec and $0.390 \cdot 10^{6}$ /sec. The values for L_o from equation 7 is 170 nH and I_o from equation 9, $6.62\ V_o$ where V_o is in volts and I_o in amperes. When $t = \tau$, the time that the current sheet is assumed to stop moving, a time that can be read from the oscillograms of dI/dt shown in Fig.5, then values of $I(\tau)$, $x(\tau)$ and $\dot{x}(\tau)$ can be found from equations 3, 4, 5 and 6 and a value for $\Delta\dot{I}(\tau+)$ from equation 2. The results of these calculations are shown in Table 1. For convenience in comparing theoretical values with experimental, $\Delta\dot{I}$ at time $t = \tau+$ is given as $\Delta\dot{I}(\tau+) \,/\, \dot{I}(t=o)$. When the discontinuity in dI/dt occured at a sufficiently fast rate the value of $\Delta\dot{I}(\tau+)$ could be measured from the oscillograms, and is given in the last column of Table 1. The agreement between the measured and calculated values of $\Delta I(\tau+)/I(t=o)$ shows that the theory can predict the sign and the order of magnitude of the discontinuity correctly.

P_o torr	V_o kV	τ μsec	$x(\tau)$ cm calculated	$x(\tau)$ cm/μsec calculated	$I(\tau)$ kA calculated	$\frac{\Delta\dot{I}(\tau+)}{I(o)}$ calculated	$\frac{\Delta\dot{I}(\tau+)}{I(o)}$ measured
o.1	7	.62	4.6	13	15.4	.o56	.o4
o.25	7	.86	5.2	11	18.8	.o53	.o4
2.5	7	1.65	4.8	4.3	21.3	.o25	
1o	7	2.6	4.4	2.o	13.7	.oo75	
o.1	1o	.51	4.6	15.5	19.2	.o58	.o3
o.25	1o	.61	4.o	12	21.8	.o51	.o5
2.5	1o	1.o2	3.2	5.2	28.9	.o32	
1o	1o	1.72	3.6	3.1	3o.o	.o19	
o.1	14	.36	3.3	16	2o.4	.o5o	.o4
o.25	14	.55	4.7	15	28.3	.o6o	.o4
2.5	14	.9o	3.6	6.9	38.3	.o39	
1o	14	1.4o	3.7	4.2	43.3	.o27	

Table 1 Snowplough analysis for plasma between electrodes

The fact that $x(\tau)$ is approximately constant irregardless of pressure and voltage merits discussion. From column 4 in Table 1, $x(\tau)$ varies between 3.2 and 5.2. From Muntenbruch's[10] measurements $x(\tau)$ should have values of up to about 9 cms. The present measurements can be brought into close agreement with Muntenbruch's results by modifying the conventional snowplough theory used for the derivation of equation 4 to 6 to take into account the difference between the flow velocity in the current sheet and the velocity of the current sheet. Denoting the ratio of these velocities by α, we have a momentum equation for the current sheet having position x and velocity $\dot{x}$ of

$$\propto m_1 x \dot{x} = \frac{1}{2} L_1 \int_o^t I^2 \, dt \qquad (11)$$

where it is assumed that α is a constant and that all gas encountered by the advancing current sheet is entrained and given a velocity that is α times the sheet front velocity. Equations of the form of equations 4, 5 and 6 can be derived on the basis of this model; the result being that the right hand side of each should be multiplied by $1/\sqrt{\alpha}$. Liebing's[13] measurements indicate a value for α that is approximately 0.5. Thus, when this model is adopted, all $x(\tau)$ and $\dot{x}(\tau)$ values given in Table 1 should be multiplied by $\sqrt{2}$. In particular the range for $x(\tau)$ then becomes $4.5 \leq x(\tau) \leq 7.4$, a range that is in closer agreement with the results of Muntenbruch. When this model is adopted, the values for $\Delta\dot{I}(\tau+)/\dot{I}(o)$ (calculated) given in Table 1 are also no longer valid. Rather the given values should be multiplied by a factor that is approximately 1.3. There is still good agreement between the calculated and measured values of $\Delta\dot{I}(\tau+)/\dot{I}(o)$.

In this Appendix it has been shown that the time, sign and magnitude of the observed discontinuity in dI/dt agrees with simple acceleration theory when the discontinuity in dI/dt is attributed to a stopping of the current sheet. Some evidence has also been found for a difference between the flow velocity in the current sheet and the sheet front velocity. It has been concluded that the current sheet probably moves a distance down the tube of less than 7.5 cm.

APPENDIX II

REFLECTED SHOCK THEORY

The three conservation equations for mass, momentum and energy when applied to describe the gas behind a shock front are

$$\rho_0 u_1 = \rho_1 (u_1 - v) \tag{11}$$

$$p_0 + \rho_0 u_1^2 = p_1 + \rho_1 (u_1 - v)^2 \tag{12}$$

$$h_0 + u_1^2/2 = h_1 + (u_1 - v)^2/2 \tag{13}$$

where the subscript o denotes conditions in front of the shock and 1 conditions behind the shock. ρ is mass density, p pressure, h enthalpy per unit mass, u_1 incident shock front velocity and v flow velocity behind the shock in laboratory coordinates. When

$$p_1 \gg p_0 \longrightarrow p_0 \approx 0 \tag{14}$$

and a parameter

$$\gamma_1 = \gamma_1(p_1, \rho_1) = h_1(p_1, \rho_1) \Big/ U_1(p_1, \rho_1) \tag{15}$$

is introduced, where U is the internal energy per unit mass of the gas, then, with the definition of the enthalpy

$$h_1 = U_1 + p_1/\rho_1 \tag{16}$$

the above equations can be solved for v/u_1

$$v/u_1 = \frac{1 + \sqrt{1 - 2 h_0 (\gamma_1^2 - 1)/u_1^2}}{\gamma_1 + 1} \tag{17}$$

The absorption of radiation in the gas ahead of a shock wave contributes to h_o as does also the passage of energy through the contact front, as proposed earlier in this report.

The three conservation equations when applied across a reflected shock are

$$\rho_2 u_2 = \rho_1 (v + u_2) \tag{18}$$

$$p_2 + \rho_2 u_2^2 = p_1 + \rho_1 (v + u_2)^2 \tag{19}$$

$$h_2 + u_2^2/2 = h_1 + (v + u_2)^2/2 \tag{20}$$

where the subscript 2 denotes conditions behind the reflected shock. $(-u_2)$ is the velocity of the front of the reflected shock. Equations (18) to (20) are completed by

$$\gamma_2(p_2, \rho_2) = h_2(p_2, \rho_2) / U_2(p_2, \rho_2) \tag{21}$$

and

$$h_2 = U_2 + p_2/\rho_2 \tag{22}$$

The desired solution to equations (11) to (16) and (18) to (22) for u_2/v (the positive root of a quadratic equation) is

$$u_2/v = -\frac{1}{2}\left[\left(u_1/v - (\gamma_2 - 1)\right) - \left(\frac{h_o}{v^2}\cdot(\gamma_2 - 1)\right)\right] + \frac{1}{2}\sqrt{\left(\frac{h_o}{v^2}\cdot(\gamma_2 - 1)\right)^2 + 2\cdot\left(\frac{h_o}{v^2}(\gamma_2 - 1)\right)\cdot\left\{2 - \left(\frac{u_1}{v}\cdot - (\gamma_2 - 1)\right)\right\} + \left(\frac{u_1}{v} + (\gamma_2 - 1)\right)^2} \tag{23}$$

This equation can also be written in the form

$$(\gamma_2 - 1) = \frac{u_2}{v + h_o \cdot \frac{v + u_2}{v(u_1 + u_2)}} \qquad (24)$$

Here it can easily be seen that the solution for $h_o = 0$ becomes

$$u_2/v \; (h_o = 0) = \gamma_2 - 1 \qquad (25)$$

which is also given by Chang[14]. The ratio of reflected front velocity to incident front velocity has also been derived by him when $h_o = 0$ to be

$$u_2/u_1 \; (h_o = 0) = 2(\gamma_2 - 1)/(\gamma_1 + 1) \qquad (26)$$

In (25) (26) the strong shock approximation is implied, that the enthalpy of the gas in front of the shock can be neglected. Equation (26) follows directly from equations (17) and (25).

Numerical solution of equations (17) and (23) for various values of γ_1, γ_2 and h_o/u_1^2 have shown that the effect of h_o on u_2/u_1 is to increase the value over that which is predicted if $h_o = 0$. For example

when $\gamma_1 = \gamma_2 = 1.4$, $\frac{u_2}{u_1}(h_o = 0) = 1/3$ and $\frac{u_2}{u_1}(2h_o(\gamma_1^2 - 1) = u_1^2) = 0.37$.

When $\gamma_1 = \gamma_2 = 1.2$, $\frac{u_2}{u_1}(h_o = 0) = 0.182$ and $\frac{u_2}{u_1}(2h_o(\gamma_1^2 - 1) = u_1^2) = 0.395$.

When $\gamma_1 = \gamma_2 = 1,14$, $\frac{u_2}{u_1}(h_o = 0) = 0.131$ and $\frac{u_2}{u_1}(2h_o(\gamma_1^2 - 1) = u_1^2) = 0.372$.

When $\gamma_1 = 1.2$, $\gamma_2 = 1.14$, $\frac{u_2}{u_1}(h_o = 0) = 0.127$ and $\frac{u_2}{u_1}(2h_o(\gamma_1^2 - 1) = u_1^2 = 0.262$.

The last ratio in each of these examples is computed for the maximum value of h_o/u_1^2 that is allowed by stable strong shock theory. This value of h_o is defined by the square root term in equation 17 being set equal to zero.

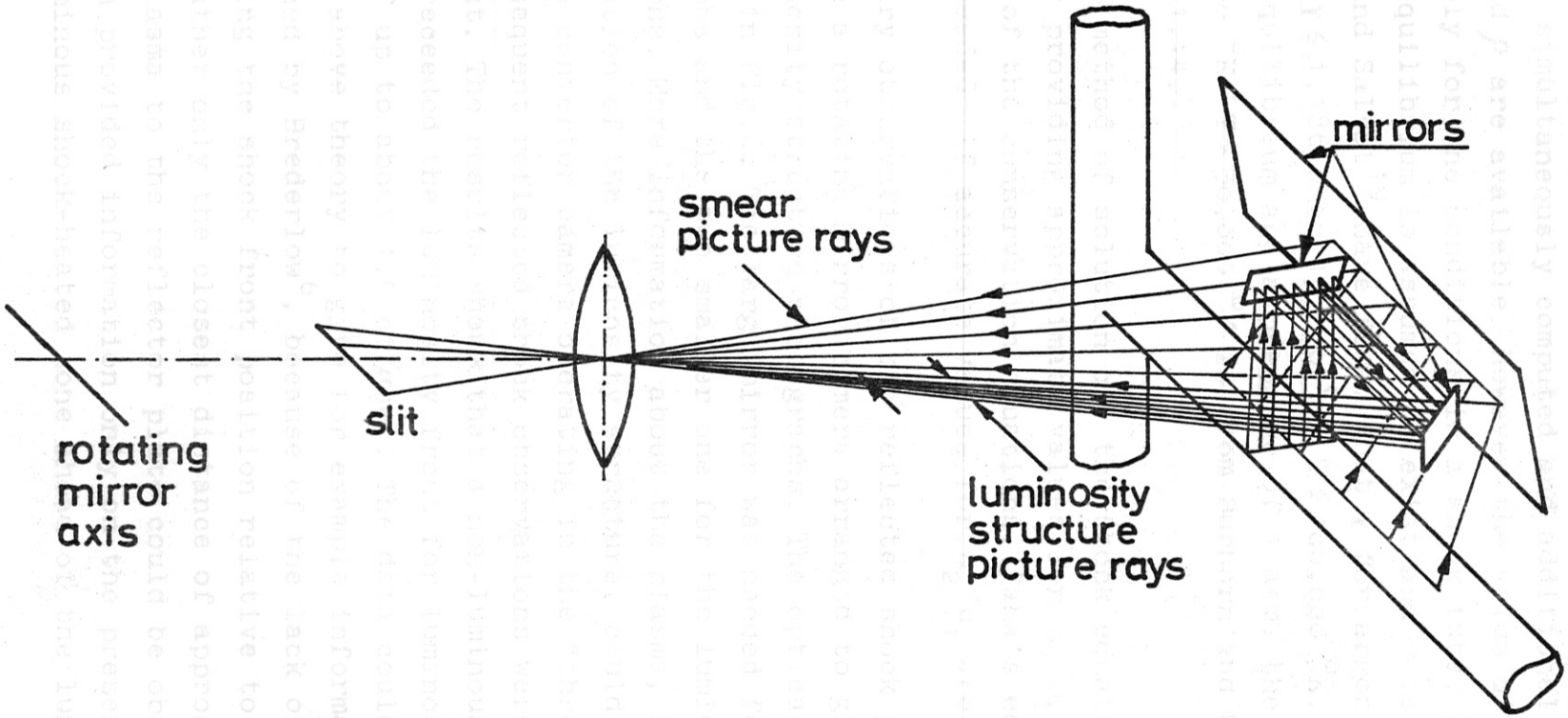

Fig. 6

JMAGE ROTATOR GEOMETRY

The above method of solution of the shock equations is not satisfactory for obtaining accurate values of u_2/u_1 unless P and ρ are simultaneously computed and additional data relating γ to P and ρ are available. However the value of γ does not vary appreciably for the conditions in a shock tube. For example when thermal equilibrium is assumed to exist and P is 1 atm, then Ahlborn and Salvat[19] have found that γ for argon is in the range of $1.14 \leq \gamma \leq 1.186$ when $15{,}000\ ^{o}K \leq T \leq 100{,}000\ ^{o}K$. For hydrogen in thermal equilibrium and a pressure of 1 atm, the values of γ when $3{,}000\ ^{o}K \leq T \leq 30{,}000\ ^{o}K$ is from Burhorn and Wienecke's[20] data $1.26 \geqslant \gamma \geqslant 1.14$.

The above method of solution of the shock equations is thus of value for providing approximate values for u_2/u_1. A machine solution of the conservation equations, Saha's equations and gas laws is needed if accurate values for u_2/u_1 are required.

Preliminary observations of the reflected shock phenomena were made with a rotating mirror camera arranged to give both smear and luminosity structure photographs. The optical system employed is shown in Fig.6. The large mirror was needed for the smear photographs and the two smaller one for the luminosity structure photographs. More information about the plasma, for example about the evolution of the luminosity structure, could be obtained with the image convertor camera operating in the "three-picture" mode. Thus subsequent reflected shock observations were made with this instrument. The results showed that a non-luminous shock-heated plasma preceeded the luminosity front for luminosity front velocities of up to about 1.5 cm/μsec. The data could not be combined with the above theory to give for example information on ρ_1/ρ_o, as obtained by Brederlow[6], because of the lack of any method for determining the shock front position relative to the luminosity front. Rather only the closest distance of approach of the luminous plasma to the reflector plate could be observed. This observation provided information only on the presence or absence of a non-luminous shock-heated zone ahead of the luminosity.

It is of interest to apply the above theory to Brederlow's[6] results. For example in his Fig.2 II a front that appears to be a reflected shock can be seen. The ratio of the reflected front velocity to the incident luminous front velocity is o.5. It is difficult to reconcile this value with the above theory because theoretical values appear to be always less than o.4, in particular considerably less when h_o is small. Even lack of equilibrium could not explain a value of o.5. The ρ_1/ρ_o curves obtained by Brederlow[6] offer evidence that h_o can be neglected (a large value of h_o markedly decreases and alters the shape of the ρ_1/ρ_o as a function of Mach number curve). Therefore it is very probable that all of the luminosity shown in this smear photograph comes from discharge-heated gases and not shock-heated gases.

APPENDIX III

SPECTROSCOPIC THEORY

The major problems considered here are the determination of the continuum intensity in a 1oo A wide interval centered on H_β and the determination of the function considered by Griem[7] for temperature measurements. Bohn[21] shows that the dependancy of the continuum intensity on wavelength in the region near the H_β line is

$$I_\nu^{Kont} \propto e^{-h\nu/kT} \qquad (21)$$

When a photomultiplier receives the integrated intensity between wavelengths λ_3 and λ_4, then the voltage output from the photomultiplier is

$$V(\lambda_4 \text{ to } \lambda_3) = K \int_{\nu_3 = c/\lambda_3}^{\nu_4 = c/\lambda_4} I_\nu^{Kont}\, S(\nu)\, d\nu \qquad (22)$$

where $S(\nu)$ is the spectral response of the photomultiplier and K is a constant that depends upon the sensitivity of the photomultiplier. In the wavelength interval used in the present experiments neither I^{Kont} nor $S(\nu)$ vary appreciably between λ_3 and λ_4. Thus

$$V(\lambda_4 \text{ to } \lambda_3) = \left\{ Kc\, S\left(\frac{\lambda_3+\lambda_4}{2}\right) I_\nu^{Kont}\left(\frac{\lambda_3+\lambda_4}{2}\right)\right\}\left\{\frac{\lambda_3-\lambda_4}{\lambda_3\lambda_4}\right\} \qquad (23)$$

where $S(\frac{\lambda_3+\lambda_4}{2})$ and $I^{Kont}(\frac{\lambda_3+\lambda_4}{2})$ denote mean values. $\lambda_3-\lambda_4$ can be expressed in terms of the exit slit width $w(\lambda_4 \text{ to } \lambda_3)$ and the reciprocal dispersion of the spectroscope averaged over the interval λ_3 to λ_4, $D(\frac{\lambda_3+\lambda_4}{2})$. Thus

$$V(\lambda_4 \text{ to } \lambda_3) = \frac{Kc\, S\left(\frac{\lambda_3+\lambda_4}{2}\right) I_\nu^{Kont}\left(\frac{\lambda_3+\lambda_4}{2}\right) w(\lambda_4 \text{ to } \lambda_3)\, D\left(\frac{\lambda_3+\lambda_4}{2}\right)}{\lambda_4\lambda_3} \qquad (24)$$

For practical measurements the H_β line intensity can be obtained from

$$I^{line} = \int_{\lambda_A}^{\lambda_B} \frac{V(\lambda_m \text{ to } \lambda_n)}{K\, S\left(\frac{\lambda_m+\lambda_n}{2}\right) w(\lambda_m \text{ to } \lambda_n)\, D\left(\frac{\lambda_m+\lambda_n}{2}\right)} d\lambda \qquad (25)$$

where again the exit slit width defines the wavelength interval λ_m to λ_n. From equation 21 it follows that the continuum intensity extrapolated to the middle of H_β is

$$I_\nu^{Kont}(H_\beta) = I_\nu^{Kont}\left(\frac{\lambda_3+\lambda_4}{2}\right) e^{-\frac{h}{kT}\left\{\nu(H_\beta) - \frac{2c}{\lambda_3+\lambda_4}\right\}} \qquad (26)$$

The function graphed by Griem[7] for temperature determinations is the ratio of the total intensity of the H_β line to the continuum intensity in a 100 ^{o}A interval centered on the line. Thus, from equations 24 to 26 it follows that

$$\frac{I^{line}(H_\beta)}{I^{Kont}(H_\beta)\,\Delta\nu} = \frac{-\,I^{line}(H_\beta)\,[\lambda(H_\beta)]^2}{I_\nu^{Kont}(H_\beta)\; c\,\Delta\lambda} \qquad (27)$$

or

$$\frac{I^{line}(H_\beta)}{I^{Kont}(H_\beta)\,\Delta\nu} = \frac{\int_0^{+\infty} \frac{V(\lambda_m \text{ to } \lambda_n)}{S\left(\frac{\lambda_m+\lambda_n}{2}\right) D\left(\frac{\lambda_m+\lambda_n}{2}\right)} d\lambda}{\frac{\Delta\lambda\,\lambda_3\lambda_4\, V(\lambda_4 \text{ to } \lambda_3) w(\lambda_m \text{ to } \lambda_n)}{[\lambda(H_\beta)]^2 S\left(\frac{\lambda_3+\lambda_4}{2}\right) w(\lambda_4 \text{ to } \lambda_3) D\left(\frac{\lambda_4+\lambda_3}{2}\right)} e^{-\frac{h}{kT}\left[\nu(H_\beta) - \frac{2c}{\lambda_3+\lambda_4}\right]}} \qquad (28)$$

where $\Delta\lambda$ = 100 ^{o}A $\triangleq \Delta\nu$.

APPENDIX IV

SCALE HEIGHT THEORY

When a mixture of gases is subjected to a constant accelerating force, a mass separation will occur. The degree of separation is decreased by such effects as unlike-particle collisions and turbulent motion. In the earths atmosphere these stabilizing effects are of sufficient importance to prevent large changes occuring in the mean molecular weight up to heights of about 2oo miles. When unlike-particle collisions and turbulence effects are neglected and a model considered that is a container filled with a mixture of gaseous chromium and hydrogen at a temperature T, then a deceleration g of the container results in mass separation governed by the equations

$$\rho_{c,h} \frac{\partial v_{c,h}}{\partial t} = - \frac{\partial P_{c,h}}{\partial \xi} - g \rho_{c,h} + \mu \frac{\partial^2 v_{c,h}}{\partial \xi^2} \qquad (29)$$

and

$$\frac{\partial \rho_{c,h}}{\partial t} + \frac{\partial (\rho v)_{c,h}}{\partial \xi} = 0 \qquad (30)$$

Here it is assumed that the coefficient of viscosity μ is independant of position in the gas, that ξ is the coordinate in the direction of motion and measured in the moving system, and that $\rho_{c,h} = \rho_{c,h}(\xi, t)$ and $v_{c,h} = v_{c,h}(\xi, t)$. The subscript c,h denotes the kind of particle being considered, i.e. chromium or hydrogen atoms. Equations 29 and 3o are thus 4 equations.

For simplicity in the calculations it will be assumed that the gas is not ionized and that the hydrogen is fully dissociated. Then

$$P_c = \rho_c RT/24 \qquad (31)$$

and

$$P_h = \rho_h RT/1 \qquad (32)$$

where $R = 8.315 \cdot 10^7$ ergs/^oK when P is in dynes/cm^2 and ρ in gms/cm^3. The full solution to equations 29 to 32 would involve machine computations. The steady state solutions are

$$\rho_c = \rho_{co}\, e^{-\frac{24 g \xi}{RT}} \tag{33}$$

$$\rho_h = \rho_{ho}\, e^{-\frac{g \xi}{RT}} \tag{34}$$

where ρ_{co} and ρ_{ho} can be determined from the initial conditions. When T=5,ooo ^{o}K and g=1o^{11} cm/sec^{2} the e-folding distances, the scale heights, given by equations 33 and 34 are respectively o.1 and 3.2 cm.

Thus the mass separation due to the deceleration of the container is large and occurs over a distance that is small compared to the dimensions of the shock tube.

APPENDIX V

PLASMA DECELERATION THEORY

In this appendix the constant momentum snowplough model for the decelerating plasma will be considered. A comparison will be made between the motion of two decelerating plasmas being driven by different driving masses. Such a model is an approximation for the case of electrode material being mixed only with the gases in the top half of the plasma. That is, we are considering the motion of the plasma in the upper half of the tube to be independant of that in the lower half. In this model the following momentum equations are valid

$$\left(\beta m_o + m_1 x_h\right) \dot{x}_h = \beta m_o \dot{x}_o \qquad (35)$$

$$\left(m_o + m_1 x_1\right) \dot{x}_1 = m_o \dot{x}_o \qquad (36)$$

where the subscript h denotes plasma being driven by the heavier mass and 1 that driven by the lighter. β is a constant and has a value greater than 1, m_o is the mass increase of each plasma per unit length of the tube, $\dot{x}_o$ is the initial velocity of each plasma and x is the axial displacement of the front of each plasma measured from the base of the electrodes.

The solutions to these equations letting $x_h(t=o)=x_1(t=o)=o$ are

$$x_h = \frac{\sqrt{(\beta m_o)^2 + 2\beta m_o \dot{x}_o t} - \beta m_o}{m_1} \qquad (37)$$

$$x_1 = \frac{\sqrt{(m_o)^2 + 2 m_o \dot{x}_o t} - m_o}{m_1} \qquad (38)$$

The separation of the plasma fronts is $x_h - x_1$. The practical problem here is to determine what the value of β would have to be to result in a value for $x_h - x_1$ of about o.5 cm when x_1=24 cm, $m_1 = 1.o4 \cdot 1o^{-6}$ g/cm, $m_o = 3.4 \cdot 1o^{-6}$ g and $m_o \dot{x}_o$=34.o gcm/sec. The position of the front of the plasma is given by χ where χ=x-1o. The value of m_1 was assumed to be equal to one-half the product

of initial density and the cross-sectional area of the shock tube, and the values of m_o and $m_o \dot{x}_o$ were obtained by methods discussed in reference 9 and using x(t) data from the streak photograph given in Brederlow's[6] Fig.2 III. The values of m_o and $m_o \dot{x}_o$ were obtained from a graph of τ/x as a function of x where τ is the time measured relative to the time when $x=o$. Thus in the problem that is being studied it is assumed that at x=1o cm both halves of the plasma have identical axial positions and velocities, but different masses. Substituting the above numerical values into equation 38 and letting $x=14$ cm gives $\tau = 4.395 \cdot 1o^{-6}$ sec. Substituting this value and other numerical values into equation 37 and letting $x_h = 14.5$ cm gives $\beta = 1.o9$. Thus a difference at x=1o cm of only 9% in the masses of the two plasmas would result in a difference of o.5 cm between the distance that the two plasmas have moved by the time that the lighter plasma has moved to x=24 cm. If only hydrogen and chromium ions were in the heavier plasma and hydrogen in the lighter, the percentage of chromium ions that would correspond to this 9% increase in mean molecular weight is o.8%. If there were only atoms of hydrogen and chromium present, the percentage of chromium atoms would be o.4%. Such a percentage of impurities could easily exist in the plasma that has been studied. For example, the spectroscopic studies have disclosed spectral lines of chromium, iron, calcium, and silicon. Therefore the above calculations provide further confirmation that heavy particles or heavier-than-average regions could be the cause of the observed luminosity structures.

REFERENCES

1 M.Cloupeau
Phys.Fluids 6, 679, 1963

2 P.Jeanmaire, H.Klingenberg and H.Reichenbach
Z.Naturforschg. 18a, 318, 1963

3 A.J.Barnard and G.D.Cormack
Proceedings of the Sixth International Conference on Ionization Phenomena in Gases, Paris 1963, to be published

4 C.T.Chang
Proceedings of the Sixth International Conference on Ionization Phenomena in Gases, Paris 1963, to be published

5 E.A.McLean, C.E.Faneuff, A.C.Kolb and H.Griem
Phys.Fluids 3, 843, 1960

6 G.Brederlow
Z.Naturforschg. 18a, 868, 1963

7 H.Griem
Proceedings of the Fifth International Conference on Ionization Phenomena in Gases, Munich 1961 (North-Holland Publishing Company, Amsterdam 1962) p.1857

8 Y.Nagakawa and K.Earnshaw
Proceedings of the Sixth International Conference on Ionization Phenomena in Gases, Paris 1963, to be published

9 G.D.Cormack
Can.Jnl.Phys. 41, 1591, 1963

* These observations and other details are discussed in the appendices

10 H.Muntenbruch
Institut für Plasmaphysik, Garching bei München, private communication

11 V.F.Kitayeva and N.N.Sobolev
Proceedings of the Fifth International Conference on Ionization Phenomena in Gases, Munich 1961 (North-Holland Publishing Company, Amsterdam 1962) p.1897

12 S.A.Ramsden and E.A.McLean
Nature 194, 761, 1962

13 L.Liebing
Phys.Fluids 6, 1035 (1), 1963

14 C.T.Chang
Phys.Fluids 4, 1085, 1961

15 N.C.Freeman
Proc.Roy.Soc.London A228, 341, 1955

16 E.J.Opik
Physics of Meteor Flight in the Atmosphere, Interscience Publishers Ltd., London, 1958, p.8

17 G.D.Cormack
Ph.D.Thesis, University of British Columbia, 1962

18 D.E.Gray
in American Institute of Physics Handbook,
McGraw Hill Book Publishing Co., Inc., 1963, pg 5-29

19 B.Ahlborn and M.Salvat
Institut für Plasmaphysik Bericht IPP 3/2, 1962

2o F.Burhorn and R.Wienecke
Zeitschr.für Physikalische Chemie, 215, 285-292, 196o

21 W.L.Bohn
Physikalisches Institut der Rheinisch-Westfälischen Technischen Hochschule Aachen PPS 1o1, 1963